Contribution from the Department of Chemistry,
University of North Carolina, Chapel Hill, North Carolina 27514

Exchange Interactions in Halide-Bridged Chains of Copper(II). $Cu(Rpy)_2X_2$

VAN H. CRAWFORD and WILLIAM E. HATFIELD*

Received September 20, 1976 AIC606831

The magnetic and spectral properties of a series of substituted pyridine complexes of copper(II) chloride and of copper(II) bromide have been determined. The bases used include 3-methyl-, 3-ethyl-, 4-methyl-, 4-ethyl-, and 4-vinylpyridine. All compounds except $Cu(4\text{-}Me(py))_2Cl_2$ exhibit Heisenberg chainlike magnetic behavior with the exchange integrals for the bromo complexes being approximately twice that observed for the chloro complexes. The J values ranged from -22.3 cm^{-1} for $Cu(3\text{-}Et(py))_2Br_2$ to -6.7 cm^{-1} for $Cu(4\text{-}Et(py))_2Cl_2$. The magnetic data for $Cu(4\text{-}Me(py))_2Cl_2$ may be interpreted in terms of an alternating-chain model with the ratio of the exchange coupling constants for a given copper(II) ion with its two nearest neighbors in the chain being 0.6.

Introduction

The linear-chain polymer $Cu(py)_2Cl_2$ has been studied extensively,[1-6] and it is generally accepted that this complex exhibits magnetic properties which are readily explained by the one-dimensional Heisenberg model. The bromide analogue also exhibits linear-chain behavior where it is found that the exchange coupling constant for $Cu(py)_2Br_2$ is greater than that of the chloride complex. The antiferromagnetic $|J|$ value for the chloride is greater than that for the bromide in the dimers $Cu(2\text{-}pic)_2X_2$,[7] and presumably, this inversion in the relative magnitudes of $|J|$ reflects the structural differences between these complexes. The crystal structures of $Cu(py)_2Cl_2$,[5] $Cu(py)_2Br_2$,[5] $Cu(4\text{-}Et(py))_2Cl_2$,[8] and $Cu(4\text{-}Vi(py))_2Cl_2$[9] (Vi = vinyl) have been reported, and a number of investigations of various properties of substituted pyridine complexes of copper(II) halides have been carried out.[10-17] To more thoroughly investigate the interactions in these complexes, a series of copper(II) halide complexes with methyl- and ethyl-substituted pyridines have been prepared and characterized, and the results of these studies are reported herein.

Experimental Section

Preparation of the Complexes. The 3-picoline (3-pic), 4-picoline (4-pic), 3-ethylpyridine (3-Et(py)), and 4-ethylpyridine (4-Et(py)) complexes with copper(II) chloride and bromide were prepared from ethanol solutions by adding, with stirring, equal volumes of 0.01 M copper(II) halide to 0.02 M substituted pyridine. Commercially available materials were of the best available grade and were used as received. The powdery precipitates were collected, washed with ethanol, and air-dried. The complexes were recrystallized slowly from either CH_2Cl_2 or $CHCl_3$. For some complexes, the brownish scum which formed during evaporation of the solvent was found to be the corresponding $Cu_4OX_6L_4$ complex which may be separated by washing the powdered material with benzene. All the complexes formed as needles, with the chloride complexes being blue and the bromide complexes being green.

The preparation of the $Cu(4\text{-}Vi(py))_2Cl_2$ complex provides an exception to this method. A powdery material forms from ethanol, as above, but it is not soluble in either $CHCl_3$ or CH_2Cl_2. The material does dissolve in dimethylformamide (DMF) to give a rich green solution, but slow evaporation does not yield crystals. After an extended period of time (several days), the color of the solution changes to a brown-black and a similar-color noncrystalline precipitate forms. This presumably is due to polymerization of the vinylpyridine. Very small crystalline needles were recovered by cooling the freshly prepared, concentrated DMF solution several days in a freezer.

The $Cu(py)_2Cl_2$ and $Cu(py)_2Br_2$ complexes were prepared by Dr. D. Y. Jeter.[1] The complexes were analyzed for copper and halide using standard volumetric techniques and/or for carbon, hydrogen, and nitrogen by Galbraith Laboratories. The differences between observed and calculated percentages were less than 0.15% for Cu, 0.2% for Cl, 0.5% for Br, and 0.3% for C, H, and N.

Magnetic Susceptibility. Magnetic susceptibilities were measured using a Princeton Applied Research Model 155 or 150A vibrating-sample magnetometer. A sphere of very pure nickel was used to calibrate the instrument; a saturation moment (for fields greater than 8000 G) of 55.01 emu/g at room temperature or 58.19 emu/g at 4.2 K was assumed. The rated accuracy of the susceptibility measurement is better than 1%. Temperatures were measured using a GaAs diode driven by a 10-μA constant-current source, and the voltage was monitored with a Dana Model 4700 digital multimeter. The working diode, located directly above the sample on the drive rod,[18] was calibrated vs. a calibrated diode supplied by Lake Shore Cryotronics, Inc. A continuous relationship between voltage and temperature was generated using a Chebyshev polynominal, and the accuracy of the temperatures is estimated to be better than 0.1%.

The magnetic field of the Westinghouse superconducting magnet was determined by measuring the voltage across the precision shunt to an accuracy of 1% with a Keithly Model 160 digital multimeter. The Ventron Model HSR-1365C electromagnet was calibrated using NMR techniques, and the 10-kG field usually used for the susceptibility determinations was accurate to better than 0.01%.

Electron Paramagnetic Resonance. The EPR spectra were recorded on a Varian E-3 using a standard insertion Dewar for the liquid nitrogen measurements. The field was read directly from the calibrated chart paper. This technique was checked using a Magnion G-502 precision gaussmeter, a Hewlett-Packard 5245L frequency counter, and a DPPH sample; the results indicated that the accuracy is better than 1% in the region used.

Electronic Spectra. The ultraviolet and visible spectra of the complexes were recorded on a Cary 14 using a mull technique; a piece of filter paper was wet with Nujol and the sample, in finely ground form, mixed into Nujol was smeared onto the paper. Filter paper wet with Nujol was used as a reference.

Results

Magnetic Properties. The temperature dependence of the corrected molar susceptibility for $Cu(3\text{-}Et(py))_2Cl_2$ is shown in Figure 1. All of the complexes, except $Cu(4\text{-}pic)_2Cl_2$ (see Discussion), exhibit similar behavior although the magnitude of the susceptibility and the temperature at the maxima differ. The data were corrected for diamagnetism and temperature-independent paramagnetism, which was assumed to be 60×10^{-6} cgsu/mol.[19] Since the susceptibilities at the lowest temperatures do not tend toward zero, the data are indicative of linear-chain behavior and the Heisenberg model is applicable. Since there are no closed-form expressions for the Heisenberg model, the values of g and J were determined from the Bonner and Fisher expressions[20]

$$|J| = kT_{max}/1.282$$

$$g = [|J|\chi_{max}/0.073\,46N\beta^2]^{1/2}$$

The data have been corrected, as described previously,[21] for the presence of a small percentage of monomeric material, which was assumed to have the same molecular weight as the sample and a temperature-independent moment of 1.9 μ_B. It is important to note that the correction has no significant effect on the values of the parameters of interest, i.e., g and J. For example, the data for $Cu(3\text{-}Et(py))_2Cl_2$ are shown in Figure

Table I. Experimental Spectral and Magnetic Results for CuL_2X_2 Complexes

X	L	⟨g⟩	J,[a] cm^{-1}	% impurity	Electronic spectra[b] λ_{max}, nm	Diamag cor[d]
Cl	py	2.13	−9.2[c]		670, 340 w, sh, 290, 255	
	3-pic	2.13	−8.9	0.3	665, 350 sh, 290, 270	185
	4-pic	2.13			635, 330 sh, 292, 256	185
	3-Et(py)	2.13	−11.9	0.5	715, 360 w, sh, 300 w, sh, 262	210
	4-Et(py)	2.13	−6.7	0.7	680, 340 sh, 292, 255	210
	4-Vi(py)	2.13	−9.1	0.4	635, 310 w, sh, 275	180
Br	py	2.13	−18.9[b]		685, 420 sh, 355 w, 320 w, 255	
	3-pic	2.12	−15.5	0.5	670, 420 sh, 355 vw, 320 w, 260	205
	4-pic	2.13	−14.8	0.5	730, 420 sh, 350 w, 320 vw, 255	205
	3-Et(py)	2.12	−22.3	0.6	685, 420 sh, 355, 320 w, 250	230
	4-Et(py)	2.12	−15.4	0.75	680, 430 sh, 355 w, 310 w, 252	230

[a] ±0.2 cm^{-1}. [b] w = weak, sh = shoulder, vw = very weak. [c] Reference 1. [d] ×10^{-6} cgsu/mol.

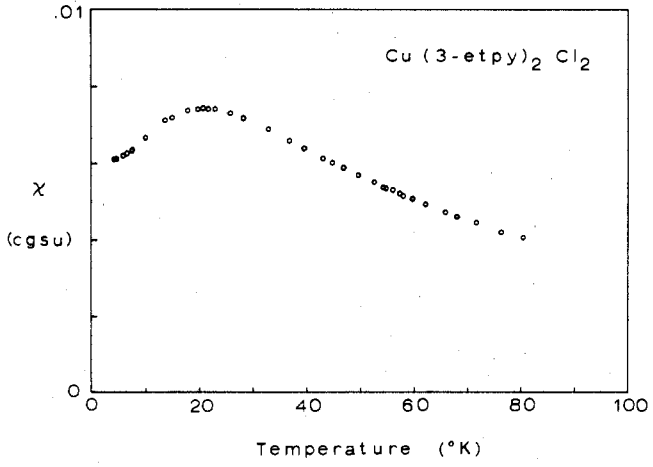

Figure 1. Magnetic susceptibility data for $Cu(3\text{-}Et(py))_2Cl_2$.

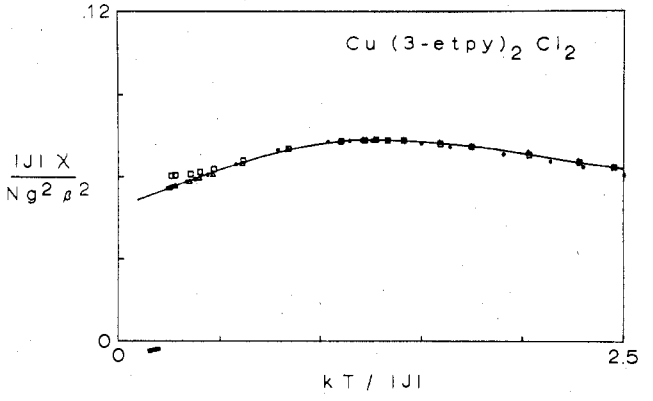

Figure 2. Magnetic susceptibility data for $Cu(3\text{-}Et(py))_2Cl_2$ in reduced coordinates: □, data as collected; △, 0.5% impurity correction; ●, 0.5% impurity correction and g set to 2.13. The solid line represents the infinite-chain extrapolation approximated from Bonner and Fisher's results.[20]

2. The squares shown in the figure are the data as collected, for which we calculate $g = 2.09$ and $J = -11.2$ cm^{-1}. The triangles represent 0.5% impurity corrected points, for which $g = 2.08$ and $J = -11.2$ cm^{-1}. The solid circles result from a calculation in which g is fixed to the EPR value and a 0.5% impurity correction is used; here $g = 2.13$ and $J = -11.9$ cm^{-1}. None of these cases is totally satisfactory with either the visual fit not being exact or the g value not agreeing precisely with the EPR experiment; but qualitative agreement with the model is quite good, and the exchange integral values should be of sufficient accuracy for valid comparisions in the series of complexes. The data for the complexes are collected in Table I, and the Heisenberg fits are shown in Figures 3 and 4. The ⟨g⟩ values determined from the EPR measurements were used as constants in the fitting processes.

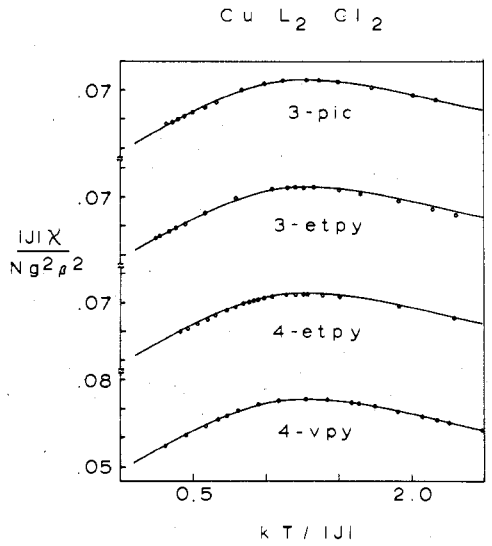

Figure 3. Magnetic susceptibility data, in reduced coordinates, for CuL_2Cl_2. The solid lines represent the infinite-chain extrapolation approximated from Bonner and Fisher's results.[20]

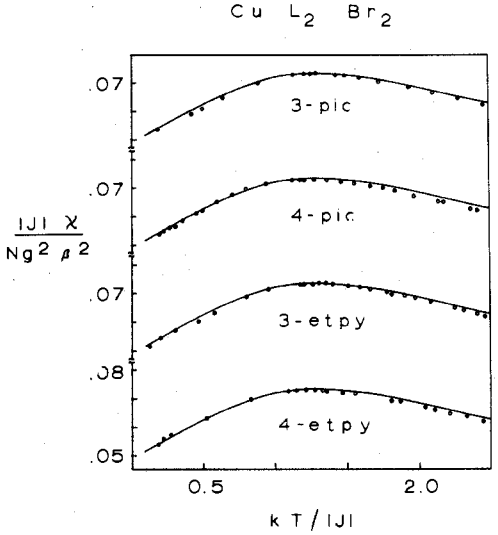

Figure 4. Magnetic susceptibility data, in reduced coordinates, for CuL_2Br_2. The solid lines represent the infinite-chain extrapolation approximated from Bonner and Fisher's results.[20]

EPR Spectra. The EPR spectra of the bromide complexes consist of one very broad resonance, while the spectra of the chloride complexes consist of a low-field resonance (about $g = 2.2$) and two closely spaced resonances near $g = 2.05$. Two exceptions are observed: in the spectrum of $Cu(3\text{-}Et(py))_2Cl_2$,

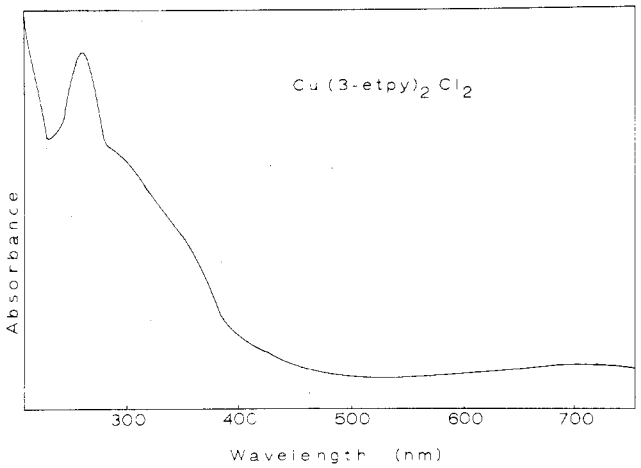

Figure 5. Electronic spectrum of $Cu(3\text{-}Et(py))_2Cl_2$.

Table II. Selected Structural Data for CuL_2X_2 Complexes

	Cu-Cu, Å	Cu-X, Å: In plane	Cu-X, Å: Out of plane	Cu-X-Cu, deg	Ref
$Cu(py)_2Cl_2$	3.85	2.30	3.03	91.52	5
$Cu(py)_2Br_2$	4.05	2.45	3.24	89.64	5
$Cu(4\text{-}Et(py))_2Cl_2$	4.00	2.28	3.22	91.8	8
$Cu(4\text{-}Vi(py))_2Cl_2$	3.91	2.31	3.10	90.05	9

the high-field peaks are not resolved and only a single broader resonance is observed, and in the spectrum of $Cu(4\text{-}Et(py))_2Cl_2$ the high-field peaks are widely separated. The spectra of all of the complexes are essentially the same at both room temperature and 77 K, with there being no significant improvement in resolution or line narrowing at the lower temperature. EPR spectra of $Cu(3\text{-pic})_2Br_2$, $Cu(3\text{-pic})_2Cl_2$, $Cu(3\text{-}Et(py))_2Cl_2$, and $Cu(4\text{-}Et(py))_2Cl_2$ are given as supplementary material.

Electronic Spectra. The spectra of all of the chloride complexes are similar to one another, as are the spectra of the bromide complexes. A representative spectrum is shown in Figure 5, and the data are collected in Table I. It is obvious that the resolution of the d–d bands is not very good; thus the values in the table for these bands are the best approximations possible. The features in the ultraviolet region of the chloride complexes are predominantly those of the substituted pyridine ligands, as described by detailed studies of the UV spectra of several of the substituted pyridines.[22] The strong bands in all of the complexes at about 255 nm are assigned to the π–π^* transitions of the ligands. The 300–420-nm region is assigned to halide-to-copper charge transfer.[17]

Discussion

In the complexes for which structural data are available,[5,8,9] the coordination at the copper consists of a trans-planar arrangement of two halides and two nitrogens from pyridines. Halides from molecules above and below the square plane occupy the out-of-plane sites yielding the familiar 4 + 2 coordination. The stacking is of such a nature as to form di-μ-halogen-bridged chains. The bonds to the out-of-plane ligands are almost perpendicular to the plane. Some structural data are shown in Table II. It is expected that the other complexes have similar structures.

The broad maxima in the magnetic susceptibility data suggested that the Heisenberg model was appropriate, and the good fits of the data with the model are regarded as justifying its use. The use of monomeric impurity corrections does not affect the magnetic parameters to any great extent, and the values of these corrections, being well below 1%, indicate that the samples are quite pure. The g values are more precisely determined from the EPR data, and differences which were observed between these values and the ones calculated from the magnetic data are not great. The intrachain exchange is antiferromagnetic in all cases, and the values of J for these complexes are of the same magnitude. Interchain interactions in $Cu(py)_2Cl_2$ have been shown to be very much smaller than the intrachain interactions.[2-4,6,16] Examination of the structural information in Table II suggests that the geometry of the bridging system is not the only factor which determines the intrachain coupling constant. However, with only four structures and three independent parameters, it is impossible to develop a definitive statement concerning structural effects on J. Even so, on the basis of observations with the hydroxo-bridged series,[23] the significant difference in bridge angles of the pyridine– and 4-vinylpyridine–copper chloride complexes would be expected to have a greater effect on the exchange integral than is observed here. This does not require that the superexchange mechanism be rejected since there are chemical differences which will affect the electron densities in the bridging portion of these chains, and these change the overlap of the bridging-ligand orbitals with copper. Since there are limited structural data, it is appropriate to consider the known chemical properties of the ligands to see if reasonable explanations can be based on the information that is available.

Table III. Selected Spectral, Magnetic, and pK_a Data for CuL_2X_2 Complexes Tabulated as X = Cl/Br

L	J, cm^{-1}	Electronic spectra, nm		pK_a[a]
3-Et(py)	−11.9/−22.3	715/685	262/250	5.70
py	−9.2/−18.9	670/685	255/255	5.17
3-pic	−8.9/−15.5	665/670	270/260	5.68
4-Et(py)	−6.7/−15.4	680/680	255/252	6.02
4-pic	.../−14.8	635/730	258/255	6.02

[a] Reference 24.

Some of the properties of these complexes are compared in Table III. Note that the magnitude of J is quite different for the two different halides and that the direction of change in the magnitude of J for the series of ligands is the same for each halide. The effect of the halide can be rationalized in terms of the larger size of the bromide ion and its "softer" nature. This implies a greater overlap of the bridging orbitals with the metal orbitals which would be expected to produce a greater antiferromagnetic coupling.

It was expected that the magnitude of J would be related to the donor properties of the pyridine ligands as measured by their pK_a values. The qualitative argument assumes that there will be increased sharing of the nitrogen donor pair of electrons with the copper(II) ion as the basicity of the ligand increases. This sharing essentially lowers the acidity (in the Lewis sense) of the copper ion for further coordination and decreases the interaction between the copper ion and the out-of-plane halides, which, of course, form the chain and transmit the superexchange interaction. This decreased interaction is reflected by the longer Cu–Cl (out-of-plane) bond distance of 3.22 Å in $Cu(4\text{-}Et(py))_2Cl_2$ as compared to the bond distance of 3.03 Å in $Cu(py)_2Cl_2$. The pK_a of pyridine is 5.17 while that of 4-ethylpyridine is 6.02. This simple argument is adequate to explain the trend in J values for all complexes except those with 3-ethylpyridine. The EPR spectrum of $Cu(3\text{-}Et(py))_2Cl_2$ (see above) suggested a somewhat different environment at the copper, and it is suggested that the steric requirements of the ethyl group in the 3 position cause an increase in the Cu–Cl–Cu angle or a decrease in the Cu–Cl distance and that these changes lead to an enhancement of the antiferromagnetic superexchange interaction.

$Cu(4\text{-pic})_2Cl_2$ also exhibits unusual magnetic behavior which is not described by Bonner and Fisher's results or by the simple dimer equation. However, the data, shown in Figure 6, have

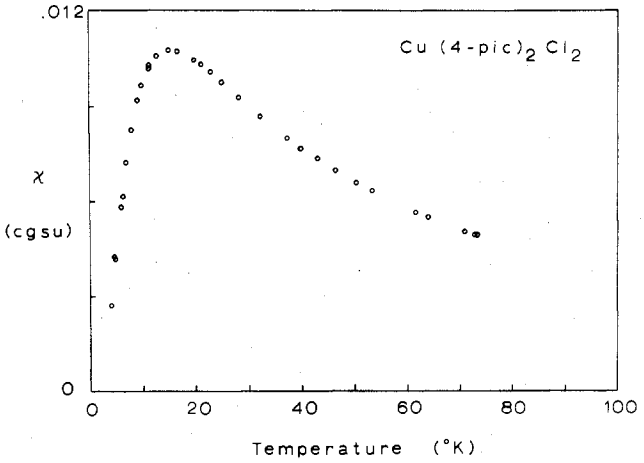

Figure 6. Magnetic susceptibility data for $Cu(4\text{-pic})_2Cl_2$.

Table IV. Copper–Halide Stretching Vibrations

Complex	ν_{Cu-X}, [a] cm^{-1}	ν_{Cu-X}, [b] cm^{-1}	ν_{Cu-L}, [b] cm^{-1}
$Cu(py)_2Br_2$	255	256	268
$Cu(4\text{-pic})_2Br_2$	255	237	257
$Cu(2\text{-pic})_2Br_2$	233	232	259
$Cu(py)_2Cl_2$	287	294	269
$Cu(4\text{-pic})_2Cl_2$	292	296	256
$Cu(2\text{-pic})_2Cl_2$	308	308	259

[a] Reference 13. [b] Reference 11.

a temperature dependence which is very similar to that reported by Duffy and Barr[25] for an alternating chain undergoing isotropic exchange coupling. Here the Hamiltonian is

$$H = 2|J|\sum_i(\hat{S}_{2i}\cdot\hat{S}_{2i-1} + \alpha\hat{S}_{2i}\cdot\hat{S}_{2i+1})$$

where J is the exchange coupling constant, $\hat{S}_i$ are the spin operators, and α can take on the values from 0.0 to 1.0; αJ is the smaller of the exchange integrals. From the Duffy–Barr results, we can estimate α to be approximately 0.6 and J to be approximately -8.5 cm^{-1}. It is unfortunate that it has not been possible to grow good nontwinned single crystals for an x-ray structure study since we expect that the structure of this complex is different from those of the other members of the series.

It was expected that the differences in bonding of the halides in the dimeric $(Cu(2\text{-pic})_2X_2$ complexes vs. the known chains $Cu(py)_2X_2$ would be reflected by the Cu–X stretching vibration in the far-infrared. Unfortunately, as shown in Table IV, there is no agreement as to the assignment of the spectral bands for these and similar complexes. Allan et al.[13] reported that $Cu(py)_2Br_2$ and $Cu(4\text{-pic})_2Br_2$ have the same ν_{Cu-Br}, and since the structure of $Cu(py)_2Br_2$ is a chain and the magnetic behavior of both complexes may be explained in terms of the Heisenberg linear-chain model, it is reasonable to assign a chain structure to $Cu(4\text{-pic})_2Br_2$. However, the data of Stieger and Ludwig[11] suggest a five-coordinate dimeric structure for $Cu(4\text{-pic})_2Br_2$. It is interesting to note that a 257-cm^{-1} band is observed by these workers for this compound but it was assigned to ν_{Cu-L}. The magnetic data suggest that the former assignment is to be preferred. Both sets of reported data suggest that $Cu(4\text{-pic})_2Cl_2$ is an intermediate case, with ν_{Cu-Cl} between those for the $Cu(py)_2Cl_2$ chain and the $Cu(2\text{-pic})_2Cl_2$ dimer. This is certainly consistent with the magnetic data which suggest alternating-chain behavior.

A recent investigation of the single-crystal EPR spectra of $Cu(py)_2Cl_2$ provided significant information about the complex,[26] and in an attempt to understand the differences

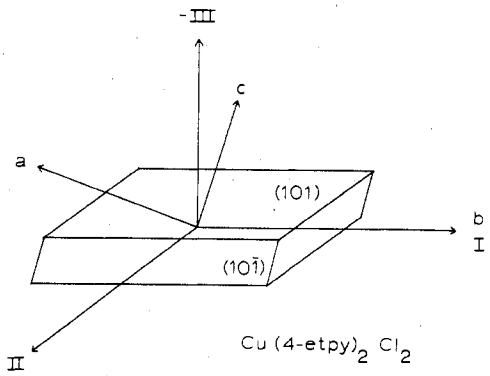

Figure 7. Morphology of a $Cu(4\text{-Et(py)})_2Cl_2$ single crystal showing crystallographic axes (a, b, c), faces, and EPR rotation axes (I, II, III).

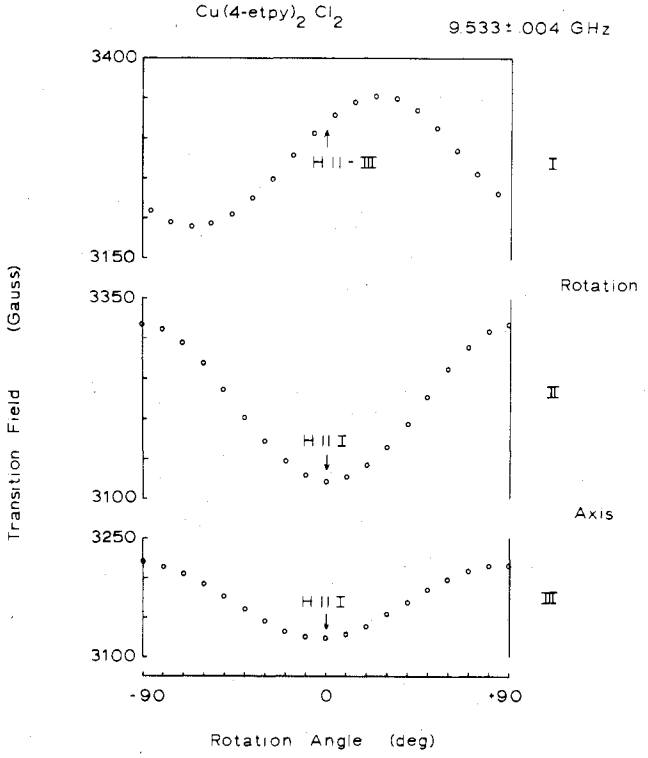

Figure 8. Transition fields for rotation around three mutually perpendicular rotation axes of the $Cu(4\text{-Et(py)})_2Cl_2$ single crystal.

observed in the powder EPR spectra of $Cu(4\text{-Et(py)})_2Cl_2$ and the other members of the series, single-crystal spectra of $Cu(4\text{-Et(py)})_2Cl_2$ were recorded. To obtain the single crystal, a sample of $Cu(4\text{-Et(py)})_2Cl_2$ was recrystallized slowly from benzene yielding very long blue needles with parallel faces. The crystal was mounted with the fiber parallel to the needle axis, and it was oriented on a Weissenberg camera (Cu radiation) using rotation and zero-level Weisenberg photographs. The room-temperature EPR spectra were recorded every 10° for rotation around three mutually perpendicular axes.

The morphology of the crystal is shown in Figure 7 where the needle axis is the crystallographic b axis, the wider faces are (101) and ($\bar{1}0\bar{1}$), and the narrower faces are (10$\bar{1}$) and ($\bar{1}$01). The crystallographic axes (a, b, c) and the three mutually perpendicular rotation axes used for the EPR spectra (I, II, III) are also shown in Figure 7. A single resonance was observed in all spectra, but the peak-to-peak derivative line width ranged from about 15–25 G for rotation around axis I (the b axis) to about 15–50 G for rotation around the other two axes. The transition fields are shown as a function of angle in Figure 8. The data, in the laboratory axis system, were

Table V. Structural Data for $Cu(py)_2Cl_2$ and $Cu(4\text{-}Et(py))_2Cl_2$

	$Cu(py)_2Cl_2$[a]	$Cu(4\text{-}Et(py))_2Cl_2$[b]
Space group	$P2_1/n$	$P2_1/c$
a, Å	16.97	11.36
b, Å	8.56	4.00[c]
c, Å	3.85[c]	17.58
β, deg	91.98	112.8
Cu–N, Å	2.00	2.00
Cu–Cl (in plane), Å	2.30	2.28
Cu–Cl (out of plane), Å	3.03	3.21
Cu–Cu, Å	3.85	4.00
Dihedral angle, deg	48.7[d]	56.1

[a] Reference 5. [b] Reference 8. [c] Chain axis. [d] Given as 46° in ref 26.

transformed to the principal **g**-tensor coordinate system by the method of Geusic and Brown,[27] using the IBM subroutine EIGEN for the matrix diagonalization.[28] The principal g values are 2.182, 2.135, and 2.033, all ±0.001. As expected, essentially the same values were obtained from the powder spectrum. The **g** tensors are labeled such that $g_1 < g_2 < g_3$, and they form a right-handed coordinate system.

Since the purpose of this investigation of $Cu(4\text{-}Et(py))_2Cl_2$ was to compare the EPR properties of the compound with those of the more studied $Cu(py)_2Cl_2$, it is important to take note of some differences in their structures. Both materials crystallize in the same monoclinic space group with the authors choosing the settings $P2_1/n$ for $Cu(py)_2Cl_2$ and $P2_1/c$ for $Cu(4\text{-}Et(py))_2Cl_2$. The structures of each are illustrated in Figure 9, and structural parameters which are necessary for this discussion are listed in Table V.

The orientation of the principal directions of the **g** tensors with respect to the molecules are also shown in Figure 9. For $Cu(4\text{-}Et(py))_2Cl_2$, within experimental error of about 5°, g_3 is collinear with the crystal b axis, which is the chain axis; g_1 is collinear with the crystal c axis, which has a similar orientation to g_2 in $Cu(py)_2Cl_2$; g_2 is about 23° away from the crystal a axis. Thus the **g** tensor for $Cu(4\text{-}Et(py))_2Cl_2$ is more closely related to the crystal-axis system than is observed for $Cu(py)_2Cl_2$.

Following the analysis of Duffy et al.[26] for $Cu(py)_2Cl_2$, with the assumption that the copper sites are of tetragonally distorted octahedral symmetry, and using the formulation of Abe and Ono,[29] the site **g** tensors are related to the crystal **g** tensors by

$$g_1^2 = g_\perp^2$$

$$g_2^2 = g_\perp^2 \cos^2 \alpha + g_\parallel^2 \sin^2 \alpha$$

$$g_3^2 = g_\perp^2 \sin^2 \alpha + g_\parallel^2 \cos^2 \alpha$$

where $g_\perp$ and $g_\parallel$ are the site g values and α is half of the angle between the tetragonal axes of the nonequivalent sites. For $Cu(4\text{-}Et(py))_2Cl_2$, using the crystal g_1, g_2, and g_3 values, the calculated results are $g_\perp = 2.033$, $g_\parallel = 2.278$, and $\alpha = 39.6°$, which is not close to being half of the 56.1° angle between the two sites. This is taken to indicate that the assumption of tetragonally distorted octahedral symmetry is inadequate for $Cu(4\text{-}Et(py))_2Cl_2$.

The discrepancy arises because the expressions are derived for an orthorhombic space group[29] where the **g** tensors are coincident with the crystal axes. For $Cu(4\text{-}Et(py))_2Cl_2$, a reasonable choice for $g_\parallel$ would be along the Cu–Cl (out of plane) direction which is about perpendicular to the plane containing the copper, nitrogens, and tightly bound chlorides. In this case $g_\perp$ would be in this plane and it is clear from Figure 9 that this is not true for g_1. Figure 9 shows that g_1 ($g_\perp$) for $Cu(py)_2Cl_2$ is also out of the pseudo square plane, and the agreement of the calculated α and half the angle between the planes of the nonequivalent sites may be fortuitous.

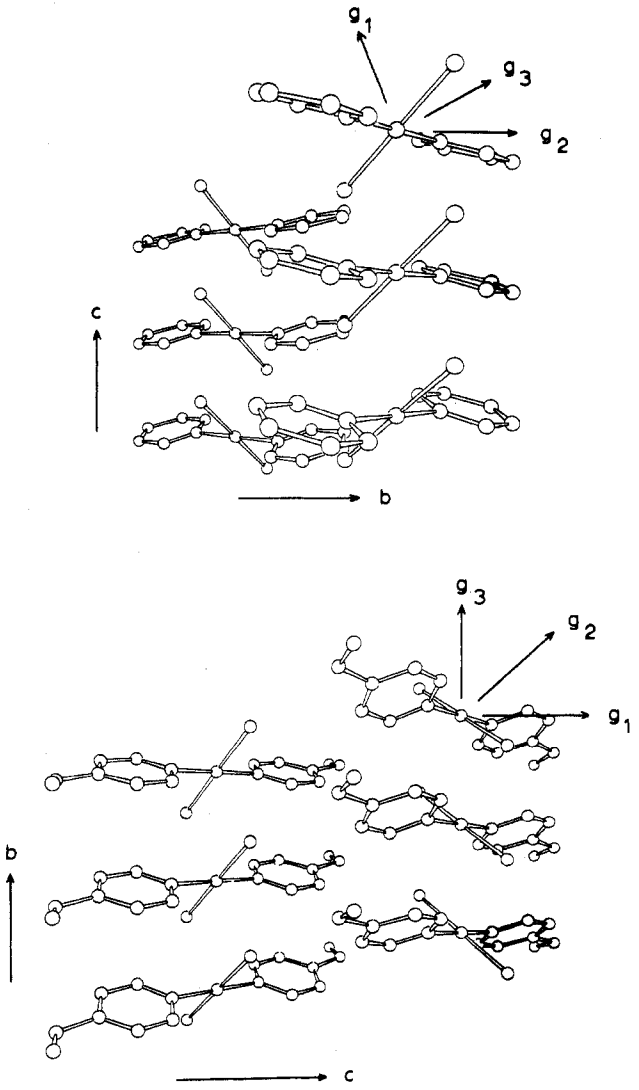

Figure 9. Structures of $Cu(py)_2Cl_2$ (top) and $Cu(4\text{-}Et(py))_2Cl_2$ (bottom) showing crystallographic axes (b and c) and crystal **g** tensors.

Since it is not possible with this approach to determine consistent values for the site **g** tensors, it is not possible to evaluate the magnitude of the interchain exchange. However since only a single resonance is observed in the EPR spectra, the expected absorptions of the nonequivalent sites must be exchange averaged. Also, since the observed line width is narrower for rotation around the crystal b axis, the chain axis, than about the other two axes, the data indicate that the effect of exchange averaging is greatest in this direction.

Acknowledgment. This research was supported by the National Science Foundation through Grant No. MPS74-11495.

Registry No. $Cu(py)_2Cl_2$, 13408-58-7; $Cu(3\text{-}pic)_2Cl_2$, 13408-59-8; $Cu(4\text{-}pic)_2Cl_2$, 14240-48-3; $Cu(3\text{-}Et(py))_2Cl_2$, 33409-25-5; $Cu(4\text{-}Et(py))_2Cl_2$, 33409-27-7; $Cu(4\text{-}Vi(py))_2Cl_2$, 15604-13-4; $Cu(py)_2Br_2$, 6845-03-0; $Cu(3\text{-}pic)_2Br_2$, 14361-57-0; $Cu(4\text{-}pic)_2Br_2$, 14361-69-4; $Cu(3\text{-}Et(py))_2Br_2$, 33409-26-6; $Cu(4\text{-}Et(py))_2Br_2$, 43070-76-4.

Supplementary Material Available: Figures showing representative EPR spectra (4 pages). Ordering information for this material is given on any current masthead page.

References and Notes

(1) D. Y. Jeter and W. E. Hatfield, *J. Inorg. Nucl. Chem.*, **34**, 3055 (1972).
(2) K. Takeda, S. Matsukawa, and T. Haseda, *J. Phys. Soc. Jpn.*, **30**, 1330 (1971).

(3) K. Andres, S. Darack, and S. L. Holt, *Solid State Commun.*, **15**, 1087 (1974).
(4) R. C. Hughes, B. Morosin, P. M. Richards, and W. Duffy, *Phys. Rev. B*, **11**, 1795 (1975).
(5) B. Morosin, *Acta Crystallogr., Sect. B*, **31**, 632 (1975).
(6) Y. Endoh, G. Shirane, R. J. Birgeneau, P. M. Richards, and S. L. Holt, *Phys. Rev. Lett.*, **32**, 170 (1974).
(7) D. Y. Jeter, D. J. Hodgson, and W. E. Hatfield, *Inorg. Chim. Acta*, **5**, 257 (1971).
(8) M. Laing and G. Carr, *J. Chem. Soc. A*, 1141 (1971).
(9) E. Horsfield and M. Laing, *Chem. Commun.*, 735 (1968); E. Horsfield, M. Sc. Thesis, University of Natal, 1968.
(10) K. E. Hyde, B. C. Quinn, and I. P. Yang, *J. Inorg. Nucl. Chem.*, **33**, 2377 (1971).
(11) H. Stieger and W. Ludwig, *Helv. Chim. Acta*, **57**, 2125 (1974).
(12) V. F. Anufrienko, A. P. Terentev, E. G. Rukhadze, and A. G. Onuchina, *Teor. Eksp. Khim.*, **2**, 412 (1966).
(13) J. R. Allan, D. H. Brown, R. H. Nuttall, and D. W. A. Sharp, *J. Chem. Soc. A*, 1031 (1966).
(14) B. K. Mohapatra and D. V. R. Rao, *Indian J. Chem.*, **9**, 715 (1971).
(15) B. K. Mohapatra, *Indian J. Chem.*, **11**, 698 (1973).
(16) V. Gamathy, K. Das, and D. Ghosh, *J. Phys. C*, **8**, 158 (1975).
(17) W. Ludwig and F. Gasser, *Helv. Chim. Acta*, **52**, 2380 (1969).
(18) R. F. Drake and W. E. Hatfield, *Rev. Sci. Instrum.*, **45**, 858 (1974).
(19) Landolt-Börnstein, "Zahlenwerte und Funktionen aus Physik, Chemie, Astronomie, Geophysik und Technik", E. König, Ed., New Series, Group II, Vol. 2, Springer-Verlag, Berlin, 1966.
(20) J. C. Bonner and M. E. Fisher, *Phys. Rev.* [*Sect.*] *A*, **135**, 640 (1964).
(21) R. P. Eckberg and W. E. Hatfield, *J. Chem. Soc., Dalton Trans.*, 616 (1975).
(22) H. P. Stephenson, *J. Chem. Phys.*, **22**, 1077 (1954).
(23) K. T. McGregor, N. T. Watkins, D. L. Lewis, R. F. Drake, D. J. Hodgson, and W. E. Hatfield, *Inorg. Nucl. Chem. Lett.*, **9**, 423 (1973).
(24) H. C. Brown and X. R. Mihm, *J. Am. Chem. Soc.*, **77**, 1723 (1955).
(25) W. Duffy, Jr., and K. P. Barr, *Phys. Rev.*, **165**, 647 (1968).
(26) W. Duffy, J. E. Venneman, D. L. Strandburg, and P. M. Richards, *Phys. Rev. B*, **9**, 2220 (1974).
(27) J. E. Geusic and L. C. Brown, *Phys. Rev.*, **112**, 64 (1956).
(28) K. T. McGregor, R. P. Scaringe, and W. E. Hatfield, *Mol. Phys.*, **30**, 1925 (1975).
(29) H. Abe and K. Ono, *J. Phys. Soc. Jpn.*, **11**, 947 (1956).

Contribution from the Department of Chemistry, The University of British Columbia, Vancouver, British Columbia, Canada, V6T 1W5

Spectroscopic and Redox Properties of Pseudotetrahedral Copper(II) Complexes. Their Relationship to Copper Proteins

H. YOKOI[1] and A. W. ADDISON*

Received September 20, 1976 AIC60691H

Visible absorption and ESR spectra and redox potentials have been examined for a series of pyrrole-2-carboxaldehyde Schiff base copper(II) complexes, whose coordination stereochemistry is distorted to varying extents from square-planar to pseudotetrahedral geometry. There are smooth correlations among d–d band energies, $A_{\parallel}$, $g_{\parallel}$, A_0, and g_0 values. As the dihedral angle between chelate rings increases from 0 through 90°, $g_{\parallel}$ increases, $|A_{\parallel}|$ decreases in an antiparallel fashion, and redox potentials shift systematically to more positive values. These observations are consistent with tetrahedral distortion at the metal binding sites of blue copper proteins.

Introduction

There is currently considerable effort being devoted to the elucidation of the composition and geometry of copper binding sites in metalloproteins.[2,5] It has long been recognized that "blue" (type I) copper sites are unusual from the inorganic chemist's viewpoint: they exhibit markedly positive Cu(II)/Cu(I) redox potentials and unique visible absorption and ESR spectra, the latter with extremely small hyperfine interactions.[6] Recently the former two properties have been studied,[7-9] Patterson and Holm having related the unusual redox properties of blue copper proteins to the electrochemical properties of selected low molecular weight copper(II) chelates.[10] Tetrahedral geometry[9,11] and the presence of sulfur donor atoms[7,8,12] have both been proposed for the blue copper sites. Quantitative conclusions with regard to the effect of stereochemistry (particularly tetrahedral distortion) on the redox potential are still in their infancy. Moreover, the paucity of redox and spectroscopic data relating to mononuclear CuN_3S and CuN_2S_2 species with nonconjugated thiolate ligands, coupled with the synthetic intractability of such systems, renders it gainful to deduce parallels between these ligand systems and CuN_4 or CuN_2O_2 centers.

Precise estimation of the degree of tetrahedral distortion of copper(II) complexes in solution is not facile, although several papers on ESR and optical absorption studies have been published,[13-16] including an application to a metal-substituted protein.[17] However, there have been a number of theoretical studies of tetrahedrally coordinated copper(II) centers and correlation with the extensive experimental studies on solid-state systems.[18-25] ESR expressions have thus been derived[21] and applied to interpretation of the spectroscopic parameters of the tetrachlorocuprate(II) ion.

Redox potentials of Cu(II)/Cu(I) systems are related to the relative thermodynamic stabilities of the two oxidation states in a given ligand environment. The factors influencing the metal-localized redox properties of copper systems have been extensively investigated by James and Williams[26] and others.[10,27]

Bis(*N*-substituted-pyrrole-2-carboxaldiminato)copper(II) complexes are of the Schiff base type yet share the pyrrole structural feature with porphyrins. They vary in stereochemistry according to the imino-N substituent, the degree of tetrahedral distortion being defined by the angle ω, as in Figure 1. Diamines yield the tetradentate species, shown as Cu(P2A$_2$-B).

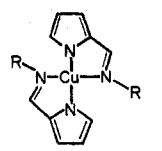

Cu(P2A-R)$_2$

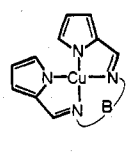

Cu(P2A$_2$B)

The first aim of this paper is to investigate the ESR and visible absorption spectra of a series of the Cu(P2A-R)$_2$ complexes with various R groups. The second is to survey the electronic features of tetrahedral distortion from the data, together with data so far known for other tetrahedrally dis-